Structural variation between neuropeptide isoforms affects function in the lobster cardiac system

Audrey J. Muscato[1#], Daniel Powell[2#,] Warsameh Bulhan[3], Evie Mackenzie[4], Alixander Pupo[5], Madeline Rolph[6], Andrew E. Christie[7], Patsy S. Dickinson[8]*

[1] Bowdoin College; ajmuscato98@gmail.com
[2] Bowdoin College; dpowell@bowdoin.edu
[3] Bowdoin College; wbulhan@bowdoin.edu
[4] Bowdoin College; evalynmackenzie@gmail.com
[5] Bowdoin College; arpupow@gmail.com
[6] Bowdoin College; madelinerolph@gmail.com
[7] University of Hawaii at Manoa; lobsterdoc@gmail.com
[8] Bowdoin College; pdickins@bowdoin.edu
* Correspondence: pdickins@bowdoin.edu
[#] Authors contributed equally to this work

[1, 2, 3, 4, 5, 6, 8] Biology Dept., Bowdoin College, 6500 College Station, Brunswick, Maine 04011

[7] Békésy Laboratory of Neurobiology, Pacific Biosciences Research Center, School of Ocean and Earth Science and Technology, University of Hawaii at Manoa, 1993 East-West Road, Honolulu, HI 96822

Declarations of interest: none

Highlights:

- AST-C isoforms elicit both similar and different physiological responses in the *H. americanus* cardiac system
- AST-C C-terminal amidation does not account for differences in physiological response to each isoform
- Single amino acid replacement in the AST-C conserved sequence is sufficient to explain many differences in physiological responses

Abstract

Neuronal responses to peptide signaling are determined by the specific binding of a peptide to its receptor(s). For example, isoforms of the same peptide family can drive distinct responses in the same circuit by having different affinities for the same receptor, by having each isoform bind to a different receptor, or by a combination of these scenarios. Small changes in peptide composition can alter the binding kinetics and overall physiological response to a given peptide. In the American lobster (*Homarus americanus*), native isoforms of C-type allatostatins (AST-Cs) usually decrease heartbeat frequency and alter contraction force. However, one of the three AST-C isoforms, AST-C II, drives a cardiac response distinct from the response elicited by the other two. To investigate the aspects of the peptide that might be responsible for these differential responses, we altered various features of each peptide sequence. Although the presence of an amide group at the end of a peptide sequence (amidation) is often essential for determining physiological function, we demonstrate that C-terminal amidation does not dictate the AST-C response in the lobster cardiac system. However, single amino acid substitution within the consensus sequence did account for many of the differences in specific response characteristics (e.g. contraction frequency or force).

Key Words: neuropeptide, isoforms, Crustacea, structure-function, allatostatin, heartbeat

1. Introduction

Pattern-generating neural networks control many behaviors, including locomotion and respiration in both vertebrates and invertebrates (Dickinson, 2006; Grillner and Wallen, 1985; Katz, 2016; Kiehn, 2006; Kiehn and Kjaerulff, 1998; Marder and Bucher, 2001; Ramirez and Baertsch, 2018). Functional flexibility in such networks allows for variable output (Blitz and Nusbaum, 2011; Gutierrez et al., 2013; White and Nusbaum, 2011), which in turn, allows neural circuits and organ systems to maintain function in response to changing environmental conditions (Flor et al., 2020; McCulloch, 2012; Powell et al., 2021; Robertson, 2004; Tang et al., 2010).

This flexibility is largely due to modulation via amines, amino acids, and peptides (Brezina, 2010; Christie et al., 2010; Jekely et al., 2018; Muñoz-Ortiz et al., 2019; Nassel and Winther, 2010; Nusbaum and Blitz, 2012; Nusbaum et al., 2017; van den Pol, 2012) . Receptor targets of neuromodulators are molecule-specific; small changes in the molecular structure of a modulatory ligand can alter the signaling response (Ericson and Haskell-Luevano, 2018; Nachman et al., 1986; Roth et al., 2006). Therefore, it is unsurprising that isoforms of the same peptide can drive unique physiological responses (Dickinson et al., 2018; Dickinson et al., 2015). For example, in the American lobster, *Homarus americanus*, there are three isoforms of C-type allatostatin (AST-C) that arise from a triplicated gene (Veenstra, 2009, 2016). Perfusion of these peptides through the heart modulates both the amplitude and frequency of the lobster heartbeat (Dickinson et al., 2018; Dickinson et al., 2009; Ma et al., 2009; Wiwatpanit et al., 2012), most often causing a decrease in cardiac contraction frequency; however, their impact on contraction amplitude is more variable (Dickinson et al., 2018; Wiwatpanit et al., 2012). Moreover, heartbeat responses to AST-C I and III are similar to one another, but both differ from the responses to

AST-C II (Dickinson et al., 2018). Although the peptide sequences of these three AST-C isoforms all differ from one another, it is not known which structural differences are responsible for the similarities and differences observed in the physiological responses.

Many neuropeptides are post-translationally modified after the final cleavage step from their pro-hormone. These modifications can include carboxyl (C)-terminal amidation, cyclization of amino (N)-terminal glutamine/glutamic acid residues, disulfide bridging between cysteine residues, and sulfation of tyrosines (Christie et al., 2010). Post-transcriptional modifications can confer bioactivity to a peptide, as is often the case with C-terminal amidation (Christie et al., 2010; Cuttitta, 1993; Merkler, 1994). For example, in the mammalian anti-opioid peptide, neuropeptide FF, C-terminal amidation is required to confer high affinity in ligand-receptor interactions (Mazarguil et al., 2001). In the cardiac ganglion of *H. americanus*, the bioactivity of myosuppressin is significantly reduced when it is not C-terminally amidated (Oleisky et al., 2022). AST-C isoforms I and III (also known as AST-C and AST-CC; Veenstra, 2016) lack C-terminal amidation and tend to alter heartbeat frequency more than the amidated isoform, AST-C II (also known as AST-CCC; Veenstra, 2016) (Dickinson et al., 2018).

Furthermore, the specific amino acid sequence of the peptide is often important in determining binding affinity for a given receptor (Ackers and Smith, 1985). For instance, in humans, a single nucleotide polymorphism (SNP) in neuropeptide S can significantly decrease bioactivity compared to the wild type sequence (Deng et al., 2013). Amino acid substitution effects on bioactivity are highly dependent on the specific amino acids being substituted (Guo et al., 2004; Ju et al., 1987; Kim et al., 2002). For example, within the crustacean red-pigment concentrating hormone (RPCH) peptide family, some changes in peptide sequence significantly alter bioactivity, whereas others have little or no effect (Marco et al., 2017).

While there are considerable differences in the non-consensus portion of each AST-C isoform, receptor binding affinity is often determined by the peptide sequence close to the C-terminal end. For AST-C isoforms, the consensus sequence is found at the C-terminus. Each AST-C isoform has a similar consensus sequence (bold below) and exhibits a disulfide bridge between the two cysteines (underlined) found within the sequence (AST-C I: pQIRYHQ**C**YFNPIS**C**F, AST-C II: SYWKQ**C**AFNAVS**C**Famide, AST-C III: GNGDGRLYWR**C**YFNAVS**C**F) (Christie et al., 2017; Dickinson et al., 2009; Ma et al., 2009; Stemmler et al., 2010; Veenstra, 2016). However, AST-C I and III are not amidated, while AST-C II is amidated. Additionally, the second amino acid in the consensus sequence of AST-C I and III is tyrosine (Y), whereas in AST-C II, this position is filled by alanine (A).

We thus hypothesized that the similarities and differences in the consensus sequence of AST-C isoforms, including amidation of the C-terminus, account for the similarities and differences in observed physiology. To test this hypothesis, we compared heartbeat responses between native and synthetic isoforms of these peptides. First, we examined whether or not amidating AST-C I and III and de-amidating AST-C II would result in a similar set of responses between isoforms. In a separate set of experiments, we replaced the alanine in the AST-C II consensus sequence with tyrosine and replaced the tyrosine in AST-C III with alanine. We also compared heartbeat responses between native and synthetic versions of these isoforms.

2. Materials & Methods

2.1 Animals and Dissection

Male and female soft and hard-shell American lobsters (*Homarus americanus*) (~500 g) were purchased from local seafood retailers in Brunswick, Bath, and Topsham, ME. Animals

were housed in tanks of recirculating seawater maintained at 10-12°C, kept on a 12hr/12hr light/dark cycle and fed chopped shrimp and squid weekly.

Lobsters were dissected and hearts recorded using techniques described previously (Dickinson et al., 2018; Stevens et al., 2009). Briefly, lobsters were anesthetized on ice for 30-60 minutes prior to dissection. The lobster heart, attached to a piece of the overlying carapace, was then removed from the body and pinned to a Sylgard 170-coated dish (Dow Corning, Midland, MI) filled with cold lobster physiological saline (composition in mM: 479.12 NaCl, 12.74 KCl, 13.67 $CaCl_2$, 20.00 $MgSO_4$, 3.91 Na_2SO_4, 11.45 Trizma base, and 4.82 maleic acid; pH 7.45). The posterior artery was cannulated, so that saline could be perfused through the heart. The saline was maintained at 10-12°C using a Peltier temperature regulator (CL-100 controller and associated SC-20 Peltier; Warner Instruments, Hampden, CT). The perfusion rate through the heart was held constant at 2.5mL/min using a Rabbit peristaltic pump (Gilson, Middleton, WI). Saline was also superfused across the top of the heart to maintain temperature.

2.2 Physiological Recordings

To measure heartbeat contractions, the anterior cardiac arteries were tied to a FT03 force transducer (Grass Natus Technologies, Pleasanton, CA); the signals were amplified using an ETH-250 Bridge amplifier (CB Sciences, Dover, NH) with a high pass filter (4 Hz), and further amplified using a Brownlee 410 amplifier (Brownlee Precision, San Jose, CA). Analog signals were digitized using a CED 1401 data acquisition interface and sampled at 10 kHz using Spike2 software (Cambridge Electronic Design; Cambridge, UK) and a Dell PC (Austin, TX). After a one-hour period of stabilization in physiological saline, AST-C isoforms were perfused through the heart for 10 minutes followed by a 50-minute saline wash. Isoforms were introduced in pseudorandom order across preparations.

2.3 Peptides

In addition to the three endogenous AST-C peptides (AST-C I: pQIRYHQCYFNPISCF, AST-C II: SYWKQCAFNAVSCFamide, AST-C III: GNGDGRLYWRCYFNAVSCF; underscores indicate disulfide bonds), five synthetic peptides were designed and used to ask how the structure of AST-C affects the effects of the peptide on the cardiac system. To test whether C-terminal amidation was responsible for the differential effects of the three AST-C isoforms, amidated versions of AST-C I and III were synthesized, as was a non-amidated version of AST-C II (**Table 1**). To test the effect of specific amino acid substitutions within the conserved portion of the AST-C II and III sequences, a synthetic peptide was created with tyrosine replacing the alanine (AST-C II Y; **Table 1**). A complementary synthetic peptide, AST-C III A, was likewise synthesized; here, alanine was substituted for tyrosine in the same location (**Table 1**). All peptides were synthesized by GenScript (Piscataway, NJ), dissolved in deionized water, and stored as a 10^{-3} M stock solution at -20°C. Immediately prior to use, all peptides were diluted to 10^{-7} M in saline.

2.4 Data Analysis and Statistics

The physiological responses of the cardiac neuromuscular system to AST-C were analyzed in Spike2 using built-in functions. The percent changes in amplitude and frequency were then calculated by determining the average amplitude and frequency over 50 heartbeats at three time-points: a baseline period before peptide perfusion, during the peak response of the heart to the peptide, and after washout (i.e., the heartbeat had returned to baseline amplitude and frequency; ~40 minutes of saline wash). Hearts were used only if they returned approximately to baseline activity after each peptide was perfused. Due to a variety of factors, including differences in intrinsic properties of each cardiac ganglion (Schulz et al., 2006; Schulz et al.,

2007) and the underlying modulatory state (Prinz et al., 2004), the baseline heartbeat frequency and contraction amplitude vary across preparations. Furthermore, perfusion of allatostatin peptides elicits a range of responses from a population of hearts (Dickinson et al., 2018). Therefore, in order to accurately compare the effect of each AST-C isoform on a given heart, as well as across the population, we compared the magnitude of response as a percent change in relation to baseline heartbeat (for both frequency and contraction force).

Statistical analysis was performed using Excel (Microsoft, Redmond, WA), Prism 8 software (GraphPad Software, San Diego, CA), SPSS (IBM, Armonk, NY), and MATLAB (Mathworks, Natick, MA). When comparing mean responses to either amidated or non-amidated peptides (3-way comparisons), a RM-ANOVA was used, followed by a Bonferroni post-hoc test of pairwise comparisons ($\alpha = 0.05$). For all RM-ANOVAs, a Sphericity test of equal variance was first calculated. If the data failed the Sphericity test, the RM-ANOVA p-value was adjusted using the Greenhouse-Geisser correction. For pair-wise comparisons of each peptide isoform (amidated vs non-amidated), a paired *t*-test was used to compare group means and a two-way Kolmogorov-Smirnov test was used to compare sampling distributions ($\alpha = 0.05$). The number of individuals in each sample varies as we only used hearts that had been exposed to all peptide isoforms for increased statistical power. When comparing native peptide isoforms to synthetic versions with single peptide substitution (**Table 1**), four pair-wise comparisons were made using both paired *t*-test and two-way Kolmogorov-Smirnov tests. To account for accumulated type II error resulting from repeated measures, we Bonferroni corrected the *p*-values of each test ($p - value \times 4$) ($\alpha = 0.05$).

3. Results

In *H. americanus* and other decapods, the pericardial organs release a milieu of neuromodulators (including peptide hormones) into the animal's hemolymph (blood equivalent). These modulators are subsequently pumped through the heart to the rest of the body. The heartbeat is generated by the cardiac ganglion, which consists of four pacemaker neurons (Small Cells) that drive five motor neurons (Large Cells) via electrical and excitatory chemical synapses (**Fig. 1A**). The resulting monophasic bursts of neuron activity drive each heartbeat contraction (**Fig. 1B**). A subset of the modulators released by the pericardial organ affect the heartbeat frequency and contraction amplitude by influencing the pacemaker and/or motor neurons, altering properties of the neuromuscular junction, directly affecting the muscle properties, or a combination of these. Therefore, to study modulation, it is important to know how a given peptide, AST-C in this study, collectively impacts the cardiac ganglion and the intact organ (i.e., the cardiac system).

3.1 Differences in AST-C amidation state do not account for physiological differences in frequency

Previous work demonstrated that AST-C isoforms I & III (non-amidated isoforms) produce distinct physiological responses from AST-C II (amidated) (Dickinson et al., 2018). To ask whether the differences in C-terminal amidation are responsible for these response differences, we synthesized isoforms of each peptide with and without C-terminal amidation (**Table 1**) and measured responses of the heart to perfusion of both native and synthetic peptides. Although the responses to the peptides varied both among animals and across peptides within an individual, the responses to the amidated and non-amidated versions of each isoform did not

differ from one another, as seen in the example recordings in **Fig 2**. Because responses to AST-C isoforms were varied and initial heartbeat frequency and amplitude were inconsistent between preparations, we compared the percent change in heartbeat frequency and amplitude elicited by perfusing each peptide isoform in a population of animals (**Methods, 2.4**). Most often, both the amidated and the non-amidated isoforms of AST-C elicited decreases in contraction frequency, and as previously described (Dickinson et al., 2018), each AST-C isoform elicited a range of responses across preparations (**Fig. 3**). This included both increase and decreases in heartbeat frequency compared to saline perfusion ($y = 0$), particularly in response to AST-C II in this set of preparations (**Fig. 3**).

Although the mean changes in contraction frequency elicited by the three amidated AST-C isoforms all differed from one another **(Fig. 3A),** the distributions of responses to the amidated isoforms of AST-C I and III were similar to one another ($p = 0.18$; **Fig. 3A**). However, the responses to both differed from the response to amidated AST-C II. Similarly, the non-amidated (native) versions of AST-C I and III elicited similar changes in contraction frequency, both of which differed from the response to AST-C II.

C-terminal amidation of AST-C I decreased the mean heartbeat frequency compared to the native form (**Fig. 3,** left plots; paired *t*-test: $p = 0.002$, $N = 47$). Similarly, removing amidation from AST-C II shifted the mean frequency toward zero (paired *t*-test: $p = 0.03$, $N = 38$), and narrowed the distribution (two sample KS test: $p = 0.002$, $N = 38$; **Fig. 3**, center plots). Interestingly, there was no difference in heartbeat frequency between amidated and non-amidated versions of AST-C III (**Fig. 3**, right plots). Thus, in contrast to the case for many peptides, differences in the amidation state of AST-C I and III relative to AST-C II did not appear to account for many of the physiological differences observed between isoforms (i.e.,

amidation of AST-C I and III did not produce responses similar to those elicited by the natively-amidated AST-C II).

3.2 Differences in amidation state do not account for physiological differences in amplitude

In general, the trends we observed in the changes in contraction amplitude elicited by amidated and non-amidated AST-C isoforms mirrored those that we observed with respect to contraction frequency. Specifically, distributions of the changes in amplitude to amidated AST-C I and III were similar ($p = 0.05$), but both differed from the responses to AST-C II **(Fig. 4A)**, as was reported in a previous study (Dickinson et al., 2018). Similarly, the non-amidated form of AST-C II did not affect contraction amplitude to the same degree as did non-amidated (native) AST-C I and III (**Fig. 4B**). However, unlike some of the changes observed in heartbeat frequency within isoforms as a consequence of amidating or de-amidating the native isoform (**Fig. 3**), altering the amidation state did not impact contraction amplitude for any isoform (**Fig. 4**).

3.3 Differences in conserved sequence may account for differences in physiological response

Because the C-terminal amidation state did not explain the differential responses to AST-C I/III and AST-C II, we next looked to differences in the conserved sequence between isoforms (**Table 1**). The conserved sequence comprises the C-terminal end of each peptide, and it is often the case that the C-terminal portion of a peptide determines ligand binding kinetics. There are two differences in the conserved sequence between the three isoforms (**Table 1).** First, AST-C II and III share an alanine (A) and valine (V) pair in positions 5 and 6 within the conserved sequence respectively, whereas AST-C I contains phenylalanine (P) and isoleucine (I) in these positions. However, this difference would only explain why the effects AST-C I differ from II

and would not explain why the AST-C III response is both similar to the response to AST-C I and different from that to AST-C II (Dickinson et al., 2018). The other difference is the presence of a tyrosine (Y) in the second position of AST-C I/III, which is held by an alanine (A) in AST-C II. Because AST-C I and III similarly alter heartbeat response (Dickinson et al., 2018) and both share a tyrosine in the second position of their consensus sequence, we chose to examine how the tyrosine/alanine difference between these sequences affects heartbeat response. Additionally, because the heartbeat response to AST-C III is not altered by AST-C III amidation (**Fig. 3 & 4**), we postulated that the substitution of tyrosine for alanine (and vice versa for AST-C II) might account for the differences observed in physiological response. To test this, we compared the heartbeat response to native isoforms of both AST-C II and III to the response to synthetic versions with the amino acid from the other peptide in position two (**Table 1**, AST-C II Y and AST-C III A). **Figure 5** shows example recordings from the same preparation in response to each native and synthetic isoform (black bars). The envelope of each trace (**Fig. 5, *left***) depicts changes in contraction amplitude and expanded traces (**Fig. 5, *right***) show changes in contraction amplitude and frequency.

3.4 The tyrosine-alanine substitution is sufficient to alter AST-C II/III contraction frequency

Interestingly, as seen in **Fig. 6A,** replacing alanine with tyrosine in AST-C II (AST-C II Y) changed the AST-C II contraction frequency mean (paired *t*-test: $p = 9.4\text{x}10^{-6}$) and distribution (two sample KS test: $p = 5.8\text{x}10^{-7}$); similarly, replacing the tyrosine in AST-C III with alanine (AST-C III A) reduced the AST-C III mean contraction frequency (paired *t*-test: $p = 9.7\text{x}10^{-9}$) and distribution (two sample KS test: $p = 1.6\text{x}10^{-12}$) (**Fig. 6B**). Furthermore, the AST-C II Y response frequency was similar to that of AST-C III (paired *t*-test: $p = 1$; two sample KS

test: $p = 1$) (**Fig. 6A** lower left vs **Fig. 6B** lower right). Although the change in heartbeat frequency was similar between AST-C II Y and AST-C III, AST-C III A elicited a different mean frequency (paired *t*-test: $p = 0.007$) and distribution (two sample KS test: $p = 0.01$) than those elicited by AST-C II (**Fig. 6A** upper left vs **Fig. 6B** upper right).

3.5 The tyrosine-alanine substitution did not alter AST-C II/III mean contraction amplitude

Unlike contraction frequency, changes in mean contraction amplitude and distribution were not altered when alanine was replaced by tyrosine in position two of the AST-C II consensus sequence (**Fig. 7A**; paired *t*-test: $p = 1$; two sample KS test: $p = 1$). Replacing tyrosine with alanine in AST-C III (AST-C III A) likewise did not alter mean contraction amplitude compared with the native form (**Fig. 7B**; paired *t*-test: $p = 0.16$); however, this substitution did narrow the distribution of responses (two sample KS test: $p = 0.002$), so that it more closely resembled the distribution elicited by AST-C II.

In comparing contraction amplitude, we observed that the two isoforms containing an alanine in position two, AST-C II and AST-C III A, elicited similar responses from the same population of hearts (**Fig. 7A** upper left vs **Fig. 7B** upper right; paired *t*-test: $p = 1$; two sample KS test: $p = 1$). Interestingly, this phenomenon does not completely hold true for the two tyrosine-containing isoforms, AST-C II Y and AST-C III. In this case, the mean contraction amplitude was different, although the distributions were similar (**Fig. 7A** lower left vs **Fig. 7B** lower right; paired *t*-test: $p = 0.01$; two sample KS test: $p = 0.31$).

4. Discussion

4.1 C-terminal amidation had little impact on AST-C bioactivity

C-terminal amidation is often a determining factor in ligand-receptor interactions and therefore bioactivity (Christie et al., 2010; Cuttitta, 1993; Merkler, 1994). For example, in the larval tobacco hornworm, *Manduca sexta*, C-terminal amidation of ecdysis-triggering hormone (ETH) is required for ecdysis (part of growth in invertebrates) (Wells et al., 2006). In the lobster, de-amidated myosuppressin has reduced bioactivity compared to the endogenous amidated form (Oleisky et al., 2022). Moreover, in vertebrate systems, endogenously amidated neuropeptide FF is five-fold more potent than the de-amidated form (Mazarguil et al., 2001).

While Dickinson et al., 2018 showed that the two non-amidated forms of AST-C (AST-C I and AST-C III) drive similar bioactivity in the lobster cardiac system, and that these responses differed from the responses to the amidated isoform, AST-C II, we found here that amidation state did not account for these differences. Although amidating or de-amidating AST-C isoforms did alter some aspects of within-isoform effects on heartbeat frequency, effects on heartbeat amplitude were similar regardless of amidation state. Furthermore, when comparing responses across isoforms for a given amidation state, the responses to AST-C II still differed from those of the other two isoforms. This suggests that C-terminal amidation is not the primary factor underlying the differential effects of AST-C I/III and AST-C II.

This finding is not unique to *H. americanus*. In crayfish, amidation of the orcokinin peptide had little effect on bioactivity (Bungart et al., 1995). Similarly, there are two forms of pituitary adenylate cyclase-activating peptide (PACAP), which modulate neurodegeneration. Although both forms of PACAP are C-terminally amidated, de-amidation of PACAP of either did little to affect bioactivity on both the rat and human PAC1 receptors (Emery et al., 2016).

4.2 Peptide sequence substitution was sufficient to alter function

Although C-terminal amidation was not responsible for the differential responses elicited by the AST-C isoforms, it is nevertheless common that the C-terminal sequence is an important determinant of ligand-receptor interactions. Our reasons for comparing sequence substitutions between AST-C II and III were three-fold. Both peptides elicited distinct heartbeat responses across the population, but they differ by only one amino acid in their consensus sequence. In contrast, AST-C II differs by two amino acids from AST-C I. Furthermore, heartbeat response to AST-C III was unaffected by amidation for both peptides. Therefore, it was reasonable to hypothesize that the difference in heartbeat response to AST-C III and AST-C II could be due to differences in their conserved peptide sequence.

It was intriguing that the difference in consensus sequence between AST-C II and III was an alanine (AST-C II) *vs.* a tyrosine (AST-C III). Alanine is a small amino acid, with a relatively small R-group (-CH_3) and is non-polar. Alanine is therefore less likely to play a role in binding affinity for a receptor, as it is unlikely to strongly interact with other molecules. Conversely, tyrosine has both an aromatic ring and a polar alcohol group. Both of these components are known to facilitate peptide-receptor interactions. It was therefore interesting to find that AST-C III A generated a change in contraction amplitude that was similar to that elicited by AST-C II and that the effect of AST-C II Y on heartbeat frequency was similar to that of AST-C III. While neither synthetic variant fully mimicked the other native isoform, these findings indicate that these amino acids are important for determining physiological response. Similar findings have been recorded in the crayfish, where a single amino acid insertion of alanine in the peptide orcokinin decreased its bioactivity and altered threshold concentration (Bungart et al., 1995). In that species, replacement of phenylalanine with tyrosine decreased orcokinin bioactivity

(Bungart et al., 1995), an interesting result as the only difference between these R-groups is tyrosine's alcohol.

The effects of single amino acid substitutions are highly dependent on the specific amino acids being substituted and their structural qualities. Marco and Gade (2010) showed that some single amino acid substitutions had little to no effect on peptide bioactivity, while others caused a substantial decrease in the bioactivity of pigment concentrating hormones in the shrimp *Palaemon pacificus* (Marco and Gade, 2010, 2015). In most systems that have been examined, the replacement of alanine with similar small amino acids and the replacement of tyrosine with other aromatic amino acids generally do not drastically affect protein function.

4.3 Differential effects on frequency and amplitude responses

In the present study, we observed that the effects of either altering amidation state or implementing single amino acid substitutions in the AST-C isoforms on heartbeat frequency could be distinct from the effects of the same changes on contraction amplitude. This can be explained by observations in AST-C modulation of the cardiac ganglion (CG). AST-C most often decreases the cycle period of the CG; in the majority of hearts, where AST-C decreases contraction amplitude, the peptide likewise decreases duty cycle (i.e. it most often affects frequency, but not burst duration (Wiwatpanit et al., 2012). While changes in CG burst period directly impact heartbeat frequency, contraction amplitude is also strongly influenced by motor neuron burst duration (Williams et al., 2013; Wiwatpanit et al., 2012). Because AST-C amidation state did not affect contraction amplitude within isoform, we predict that amidation likely does not affect CG burst duration. However, burst duration might be altered by single amino-acid

substitution, as AST-C II Y and AST-C III drive different contraction amplitudes in the same population of hearts.

4.4 Structure-Activity Relationship of C-type Allatostatins

The current study helped elucidate which structural elements of AST-C are responsible for the differential responses of the lobster heartbeat to the AST-C isoforms (Dickinson et al., 2018). While the differential responses of the AST-C isoforms can be partially explained by a single amino acid in the conserved sequence of the peptide, it is possible that differences found in the non-consensus sequence also play a role in receptor affinity. Much of this region differs substantially among the three AST-C isoforms. However, there is one other amino acid that is identical in AST-C's I and III, but different in AST-C II. Specifically, the third to last amino acid in the non-consensus sequence of AST-C I and III is a tyrosine, whereas this position is occupied by tryptophan (W) in AST-C II. Furthermore, it remains a possibility that C-terminal amidation and consensus sequence together determine bioactivity, since we only tested one or the other individually.

Further work is needed to fully explain the differences between responses to peptide isoforms. Because binding affinity could be influenced by a combination of amidation state and consensus sequence, future experiments could examine effects of synthetic AST-C isoforms with altered C-terminal amidation and amino acid substitution. However, the findings presented here further our understanding of structure-activity relationships of neuropeptides and their bioactivity in pattern generating networks.

Funding: This work was supported by the National Science Foundation [IOS-1354567 and IOS-1353023], the National Institutes of Health [P20GM0103423 from NIGMS], the Arnold and Mabel Beckman Foundation, and the Henry L. and Grace Doherty Charitable Foundation.

References

Ackers, G.K., Smith, F.R., 1985. Effects of site-specific amino acid modification on protein interactions and biological function. Annu Rev Biochem 54, 597-629.

Blitz, D.M., Nusbaum, M.P., 2011. Neural circuit flexibility in a small sensorimotor system. Curr Opin Neurobiol 21(4), 544-552.

Brezina, V., 2010. Beyond the wiring diagram: signalling through complex neuromodulator networks. Philos Trans R Soc Lond B Biol Sci 365(1551), 2363-2374.

Bungart, D., Kegel, G., Burdzik, S., Keller, R., 1995. Structure-activity relationships of the crustacean myotropic neuropeptide orcokinin. Peptides 16(2), 199-204.

Christie, A.E., Roncalli, V., Cieslak, M.C., Pascual, M.G., Yu, A., Lameyer, T.J., Stanhope, M.E., Dickinson, P.S., 2017. Prediction of a neuropeptidome for the eyestalk ganglia of the lobster *Homarus americanus* using a tissue-specific *de novo* assembled transcriptome. Gen Comp Endocrinol 243, 96-119.

Christie, A.E., Stemmler, E.A., Dickinson, P.S., 2010. Crustacean neuropeptides. Cell Mol Life Sci 67(24), 4135-4169.

Cuttitta, F., 1993. Peptide amidation: signature of bioactivity. Anat Rec 236(1), 87-93, 172-173; discussion 193-175.

Deng, C., He, X., Hsueh, A.J., 2013. A single-nucleotide polymorphism of human neuropeptide s gene originated from Europe shows decreased bioactivity. PLoS One 8(12), e83009.

Dickinson, P.S., 2006. Neuromodulation of central pattern generators in invertebrates and vertebrates. Curr Opin Neurobiol 16(6), 604-614.

Dickinson, P.S., Armstrong, M.K., Dickinson, E.S., Fernandez, R., Miller, A., Pong, S., Powers, B., Pupo Wiss, A., Stanhope, M.E., Walsh, P.J., Wiwatpanit, T., Christie, A.E., 2018. Three members of a peptide family are differentially distributed and elicit differential state-dependent responses in a pattern generator-effector system. J Neurophysiol 119(5), 1767-1781.

Dickinson, P.S., Calkins, A., Stevens, J.S., 2015. Related neuropeptides use different balances of unitary mechanisms to modulate the cardiac neuromuscular system in the American lobster, *Homarus americanus*. J Neurophysiol 113(3), 856-870.

Dickinson, P.S., Wiwatpanit, T., R., G.E., J., A.R., Stevens, J.S., Cashman, C.R., Stemmler, E.A., Christie, A.E., 2009. Identification of SYWKQCAFNAVSCFamide: a broadly conserved crustacean C-type allatostatin-like peptide with both neuromodulatory and cardioactive properties. J Exp Biol 212(Pt 8), 1140-1152.

Emery, A.C., Alvarez, R.A., Abboud, P., Xu, W., Westover, C.D., Eiden, M.V., Eiden, L.E., 2016. C-terminal amidation of PACAP-38 and PACAP-27 is dispensable for biological activity at the PAC1 receptor. Peptides 79, 39-48.

Ericson, M.D., Haskell-Luevano, C., 2018. A review of single-nucleotide polymorphisms in orexigenic neuropeptides targeting G protein-coupled receptors. ACS chemical neuroscience 9(6), 1235-1246.

Flor, K.C., Barnett, W.H., Karlen-Amarante, M., Molkov, Y.I., Zoccal, D.B.J.T.J.o.p., 2020. Inhibitory control of active expiration by the Bötzinger complex in rats. 598(21), 4969-4994.

Grillner, S., Wallen, P., 1985. Central pattern generators for locomotion, with special reference to vertebrates. Annu. Rev. Neurosci. 8(1), 233-261.

Guo, H.H., Choe, J., Loeb, L.A., 2004. Protein tolerance to random amino acid change. Proc Natl Acad Sci U S A 101(25), 9205-9210.

Gutierrez, G.J., O'Leary, T., Marder, E., 2013. Multiple mechanisms switch an electrically coupled, synaptically inhibited neuron between competing rhythmic oscillators. Neuron 77(5), 845-858.

Jekely, G., Melzer, S., Beets, I., Kadow, I.C.G., Koene, J., Haddad, S., Holden-Dye, L., 2018. The long and the short of it - a perspective on peptidergic regulation of circuits and behaviour. J Exp Biol 221(Pt 3).

Ju, G., Collins, L., Kaffka, K.L., Tsien, W.H., Chizzonite, R., Crowl, R., Bhatt, R., Kilian, P.L., 1987. Structure-function analysis of human interleukin-2. Identification of amino acid residues required for biological activity. J Biol Chem 262(12), 5723-5731.

Katz, P.S., 2016. Phylogenetic plasticity in the evolution of molluscan neural circuits. Curr Opin Neurobiol 41, 8-16.

Kiehn, O., 2006. Locomotor circuits in the mammalian spinal cord. Annu. Rev. Neurosci. 29, 279-306.

Kiehn, O., Kjaerulff, O., 1998. Distribution of central pattern generators for rhythmic motor outputs in the spinal cord of limbed vertebrates. Ann N Y Acad Sci 860, 110-129.

Kim, J.E., Jeong, H.W., Nam, J.O., Lee, B.H., Choi, J.Y., Park, R.W., Park, J.Y., Kim, I.S., 2002. Identification of motifs in the fasciclin domains of the transforming growth factor-beta-induced matrix protein betaig-h3 that interact with the alphavbeta5 integrin. J Biol Chem 277(48), 46159-46165.

Ma, M., Szabo, T.M., Jia, C., Marder, E., Li, L., 2009. Mass spectrometric characterization and physiological actions of novel crustacean C-type allatostatins. Peptides 30(9), 1660-1668.

Marco, H.G., Gäde, G., 2010. Biological activity of the predicted red pigment-concentrating hormone of *Daphnia pulex* in a crustacean and an insect. Gen Comp Endocrinol 166(1), 104-110.

Marco, H.G., Gäde, G., 2015. Structure-activity relationship of adipokinetic hormone analogs in the striped hawk moth, *Hippotion eson*. Peptides 68, 205-210.

Marco, H.G., Verlinden, H., Vander Broeck, J., Gäde, G., 2017. Characterisation and pharmacological analysis of a crustacean G protein-coupled receptor: the red pigment-concentrating hormone receptor of *Daphnia pulex*. *Sci Rep* **7,** 6851.

Marder, E., Bucher, D., 2001. Central pattern generators and the control of rhythmic movements. Curr Biol 11(23), R986-996.

Mazarguil, H., Gouarderes, C., Tafani, J.A., Marcus, D., Kotani, M., Mollereau, C., Roumy, M., Zajac, J.M., 2001. Structure-activity relationships of neuropeptide FF: role of C-terminal regions. Peptides 22(9), 1471-1478.

McCulloch, P.F., 2012. Animal models for investigating the central control of the mammalian diving response. Front Physiol 3, 169.

Merkler, D.J., 1994. C-terminal amidated peptides: production by the in vitro enzymatic amidation of glycine-extended peptides and the importance of the amide to bioactivity. Enzyme Microb Technol 16(6), 450-456.

Muñoz-Ortiz, J., Muñoz-Ortiz, E., López-Meraz, L., Beltran-Parrazal, L., Morgado-Valle, C., 2019. The pre-Bötzinger complex: Generation and modulation of respiratory rhythm. Neurología (English Edition) 34(7), 461-468.

Nachman, R.J., Holman, G.M., Cook, B.J., 1986. Active fragments and analogs of the insect neuropeptide leucopyrokinin: structure-function studies. Biochem Biophys Res Commun 137(3), 936-942.

Nassel, D.R., Winther, A.M., 2010. *Drosophila* neuropeptides in regulation of physiology and behavior. Prog Neurobiol 92(1), 42-104.

Nusbaum, M.P., Blitz, D.M., 2012. Neuropeptide modulation of microcircuits. Curr Opin Neurobiol 22(4), 592-601.

Nusbaum, M.P., Blitz, D.M., Marder, E., 2017. Functional consequences of neuropeptide and small-molecule co-transmission. Nat Rev Neurosci 18(7), 389-403.

Oleisky, E.R., Stanhope, M.E., Hull, J.J., Dickinson, P.S., 2022. Isoforms of the neuropeptide myosuppressin differentially modulate the cardiac neuromuscular system of the American lobster, *Homarus americanus*. J Neurophysiol 127(3), 702-713.

Powell, D., Haddad, S.A., Gorur-Shandilya, S., Marder, E., 2021. Coupling between fast and slow oscillator circuits in *Cancer borealis* is temperature-compensated. Elife 10, e60454.

Prinz, A.A., Bucher, D., Marder, E., 2004. Similar network activity from disparate circuit parameters. Nature Neuroscience 7(12), 1345-1352.

Ramirez, J.M., Baertsch, N.A., 2018. The dynamic basis of respiratory rhythm generation: one breath at a time. Annu Rev Neurosci 41, 475-499.

Robertson, R.M., 2004. Thermal stress and neural function: adaptive mechanisms in insect model systems. Journal of Thermal Biology 29(7), 351-358.

Roth, A.L., Marzola, E., Rizzi, A., Arduin, M., Trapella, C., Corti, C., Vergura, R., Martinelli, P., Salvadori, S., Regoli, D., 2006. Structure-activity studies on neuropeptide S: identification of the amino acid residues crucial for receptor activation. Journal of Biological Chemistry 281(30), 20809-20816.

Schulz, D.J., Goaillard, J.M., Marder, E., 2006. Variable channel expression in identified single and electrically coupled neurons in different animals. Nature Neuroscience 9(3), 356-362.

Schulz, D.J., Goaillard, J.M., Marder, E.E., 2007. Quantitative expression profiling of identified neurons reveals cell-specific constraints on highly variable levels of gene expression. Proc Natl Acad Sci U S A 104(32), 13187-13191.

Stemmler, E.A., Bruns, E.A., Cashman, C.R., Dickinson, P.S., Christie, A.E., 2010. Molecular and mass spectral identification of the broadly conserved decapod crustacean neuropeptide pQIRYHQCYFNPISCF: the first PISCF-allatostatin (*Manduca sexta*- or C-type allatostatin) from a non-insect. Gen Comp Endocrinol 165(1), 1-10.

Stevens, J.S., Cashman, C.R., Smith, C.M., Beale, K.M., Towle, D.W., Christie, A.E., Dickinson, P.S., 2009. The peptide hormone pQDLDHVFLRFamide (crustacean myosuppressin) modulates the *Homarus americanus* cardiac neuromuscular system at multiple sites. J Exp Biol 212(Pt 24), 3961-3976.

Tang, L.S., Goeritz, M.L., Caplan, J.S., Taylor, A.L., Fisek, M., Marder, E., 2010. Precise temperature compensation of phase in a rhythmic motor pattern. PLoS Biol 8(8).

van den Pol, A.N., 2012. Neuropeptide transmission in brain circuits. Neuron 76(1), 98-115.

Veenstra, J.A., 2009. Allatostatin C and its paralog allatostatin double C: the arthropod somatostatins. Insect Biochem Mol Biol 39(3), 161-170.

Veenstra, J.A., 2016. Allatostatins C, double C and triple C, the result of a local gene triplication in an ancestral arthropod. Gen Comp Endocrinol 230-231, 153-157.

Wells, C., Jr., Aparicio, K., Salmon, A., Zadel, A., Fuse, M., 2006. Structure-activity relationship of ETH during ecdysis in the tobacco hornworm, *Manduca sexta*. Peptides 27(4), 698-709.

White, R.S., Nusbaum, M.P., 2011. The same core rhythm generator underlies different rhythmic motor patterns. J Neurosci 31(32), 11484-11494.

Williams, A.H., Calkins, A., O'Leary, T., Symonds, R., Marder, E., Dickinson, P.S., 2013. The neuromuscular transform of the lobster cardiac system explains the opposing effects of a neuromodulator on muscle output. J Neurosci 33(42), 16565-16575.

Wiwatpanit, T., Powers, B., Dickinson, P.S., 2012. Inter-animal variability in the effects of C-type allatostatin on the cardiac neuromuscular system in the lobster *Homarus americanus*. J Exp Biol 215(Pt 13), 2308-2318.

Figure & Tables

Table 1. Sequences of the endogenous (rows 1-3) and synthetic (rows 4-8) AST-C isoforms used. Bolded amino acids represent the conserved peptide sequences. Underlined cystine residues indicate a disulfide bridge. Amidated isoforms AST-C I and AST-C III are indicated with a red 'a'. For AST-C II the amino acid change from alanine to tyrosine (Y) is shown in purple, and for AST-C III the amino acid change from tyrosine to alanine (A) is shown in blue.

Isoform	Sequence
AST-C I	pQIRYHQ**CYFNPISCF**
AST-C II	SYWKQ**CAFNAVSCF**a
AST-C III	GNGDGRLYWR**CYFNAVSCF**
AST-C I amidated (AST-C I-a)	pQIRYHQ**CYFNPISCF**a
AST-C II non-amidated (AST-C II-na)	SYWKQ**CAFNAVSCF**
AST-C III amidated (AST-C III-a)	GNGDGRLYWR**CYFNAVSCF**a
AST-C II Y	SYWKQ**CYFNAVSCF**a
AST-C III A	GNGDGRLYWR**CAFNAVSCF**

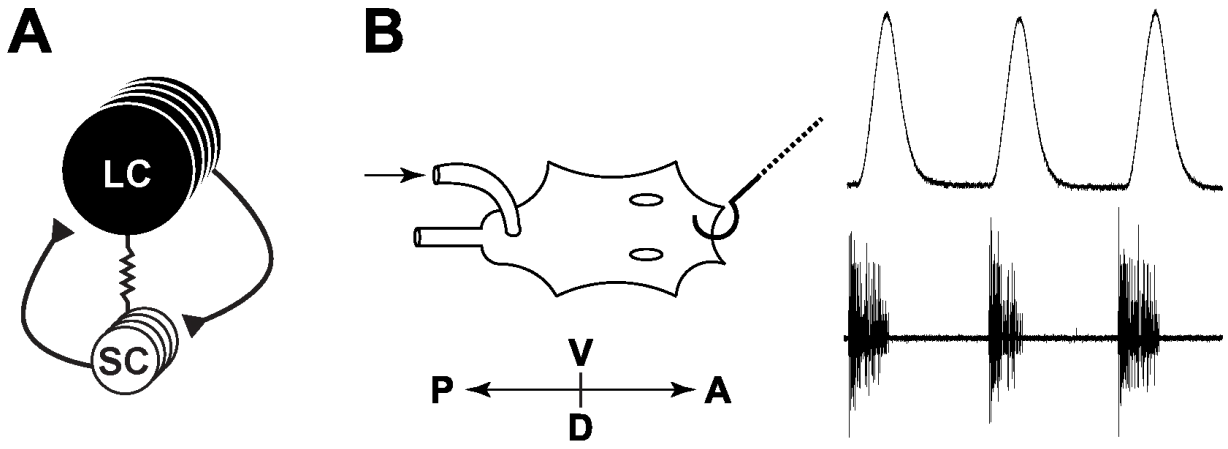

Figure 1. Schematic of the cardiac ganglion and experimental setup. (A) Connectivity diagram of the cardiac ganglion (CG). Four pacemaker neurons (Small Cells, SCs) drive five motor neurons (Large Cells, LCs) via both electrical and excitatory chemical synapses, depicted here as a resistor symbol and lines with triangles respectively. All neurons are electrically coupled. This connectivity produces a single-phase output in the form of discrete action potential bursts **(B;** lower trace**)**. **(B)** A cartoon of the lobster heart demonstrating the experimental set-up. Compass is oriented such that the abscissa is posterior (P)/anterior (A) and the ordinate is dorsal (D)/ventral (V). The hook shown at the anterior end of the heart denotes the location at which the force transducer samples the heartbeat force. The dotted line signifies the transition between force detection and the recorded heartbeat trace (upper trace). Below the heartbeat trace is a matched physiological extracellular recording from the CG demonstrating the phase locking between neuron impulse bursts and heartbeat contractions. The sternal artery (arrow) is cannulated for perfusion.

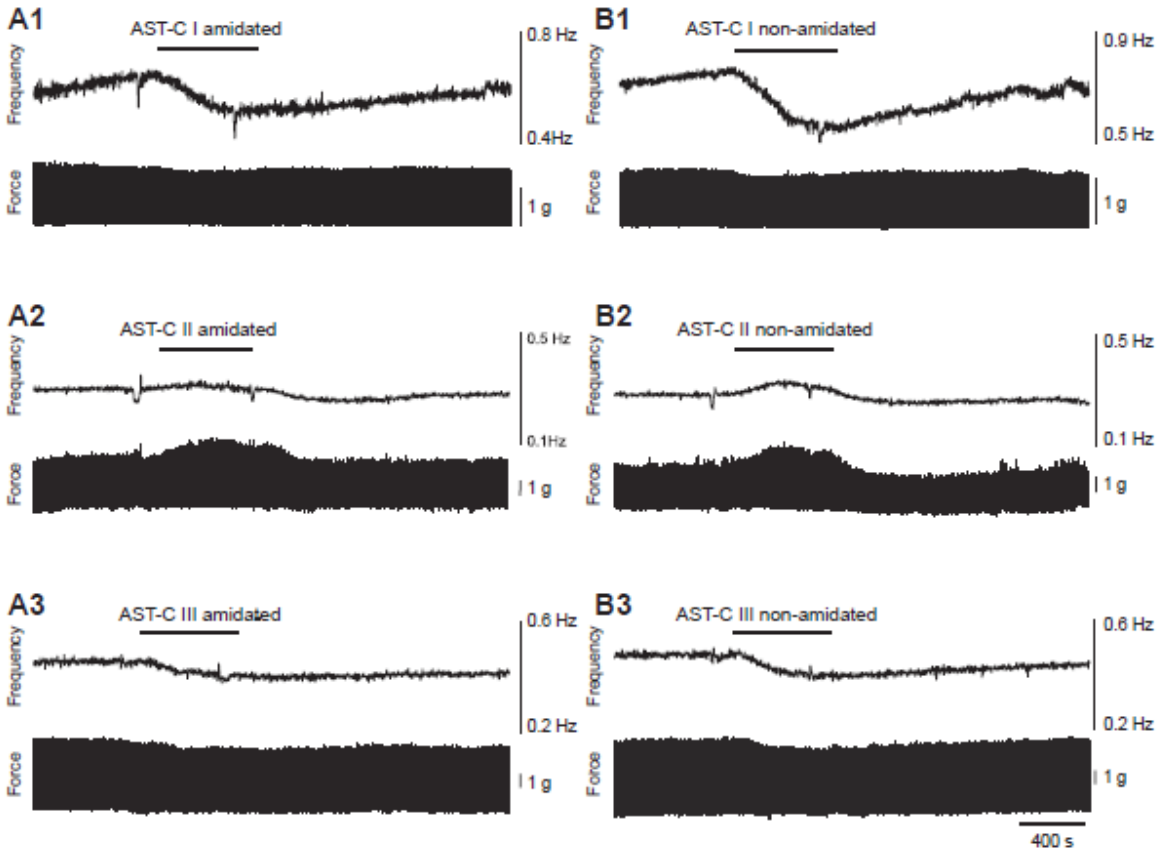

Figure 2. Compressed sample recordings of the lobster heartbeat in response to AST-C amidated and non-amidated isoforms. Recordings for each amidated **(A1, A2, A3)** and non-amidated **(B1, B2, B3)** AST-C isoform are from the same heart. Heartbeat frequency (instantaneous) is plotted above each trace. Black bars above each recording indicate peptide perfusion duration. Note that heartbeat responses within preparations differ between AST-C isoforms, but that there is little difference in the responses to the amidated and non-amidated versions of each isoform.

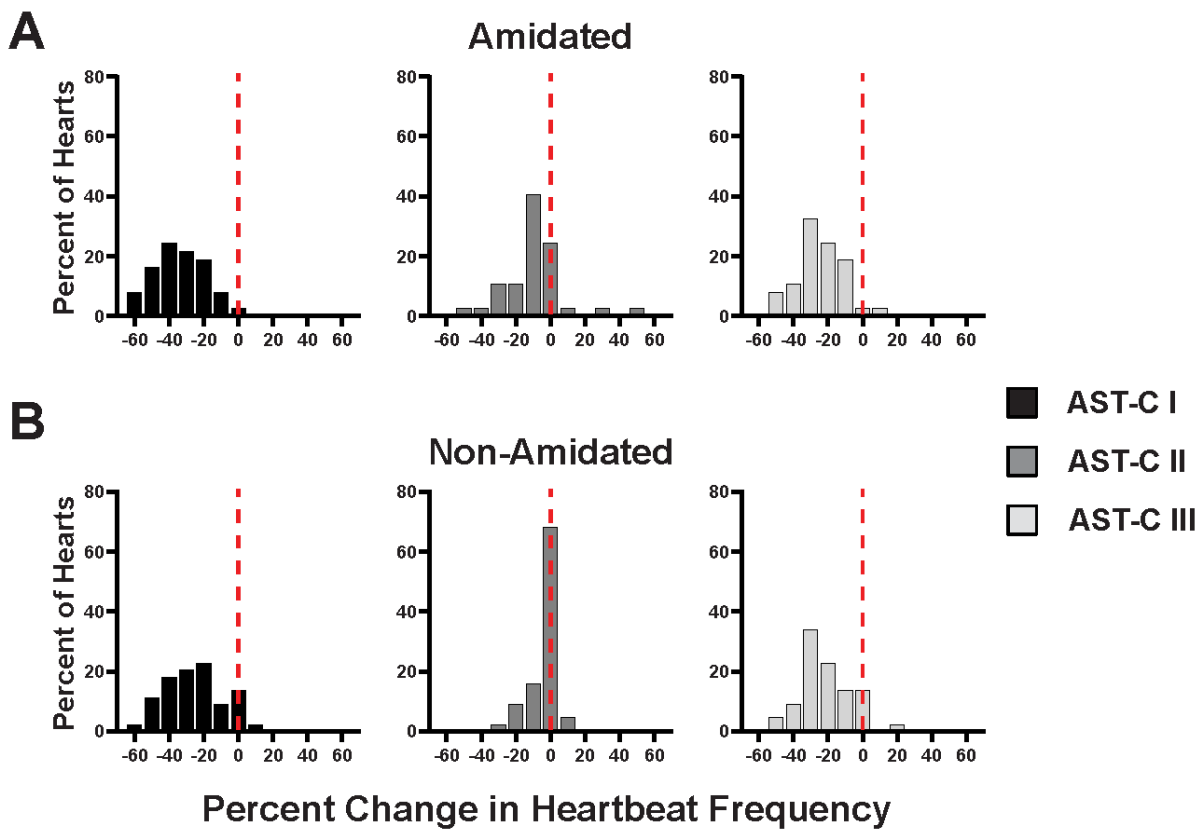

Figure 3. Distributions of heart contraction frequency in response to amidated and non-amidated AST-C isoforms. (A) Histograms of the change in heartbeat frequency from control (saline) for each amidated AST-C isoform. The red dashed line indicates $y = 0$. While AST-C isoforms generally decreased heartbeat frequency, the extent to which each isoform slowed the heartbeat was different (Mean ± SD: AST-C I: -33.72 ± 14.7 Hz, AST-C II: -9.70 ± 16.9 Hz, AST-C III: -24.34 ± 13.5 Hz; RM-ANOVA: $p < 0.0001$; Bonferroni post-hoc: I vs II: $p < 0.0001$; I vs III: $p = 0.006$; II vs III: $p < 0.0001$; $N = 37$). Distributions were compared using pairwise two-way KS tests: AST-C I vs. II: $p = 5.8\text{x}10^{-5}$; I vs. III: $p = 0.02$; II vs. III: $p = 0.18$. **(B)** Same as (**A**) but showing changes in heartbeat frequency in response to non-amidated AST-C isoforms. For non-amidated isoforms, only the heartbeat response to AST-C II was different from I & III (AST-C I: -26.95 ± 15.9 Hz, AST-C II: -4.62 ± 15.9 Hz, AST-C III: -20.37 ± 15.6 Hz; RM-ANOVA: $p < 0.0001$; Bonferroni post-hoc: I vs II: $p < 0.0001$; I vs III: $p = 0.10$; II vs III: $p < 0.0001$; $N = 44$). Distributions were compared using pairwise two-way KS tests: AST-C I vs. II: $p = 2.2\text{x}10^{-9}$; I vs. III: $p = 0.19$; II vs. III: $p = 3.6\text{x}10^{-8}$. Each AST-C isoform was compared pairwise between amidated and non-amidated versions. The amidated versions of both AST-C I and II did alter the change in heartbeat frequency compared to the non-amidated forms (AST-C I: amidated: -34.68 ± 16.0 Hz, non-amidated: -26.36 ± 15.8 Hz; paired *t*-test: $p = 0.002$, $N = 47$; AST-C II: amidated: -9.84 ± 16.7 Hz, non-amidated: -4.31 ±7.9 Hz; paired *t*-test: $p = 0.031$, $N = 45$; AST-C III: amidated: -24.59 ± 13.4 Hz, non-amidated: -20.80 ± 14.8 Hz; paired *t*-test: $p = 0.14$, $N = 38$). Distributions of amidated and non-amidated versions of AST-C I and III were not different (AST-C I: two-sample KS test: $p = 0.08$, $N = 47$; AST-C III: two-sample KS test: $p = 0.50$, $N = 45$); however, distributions of amidated and non-amidated versions of AST-C II were different (AST-C II: two-sample KS test: $p = 0.0022$, $N = 38$).

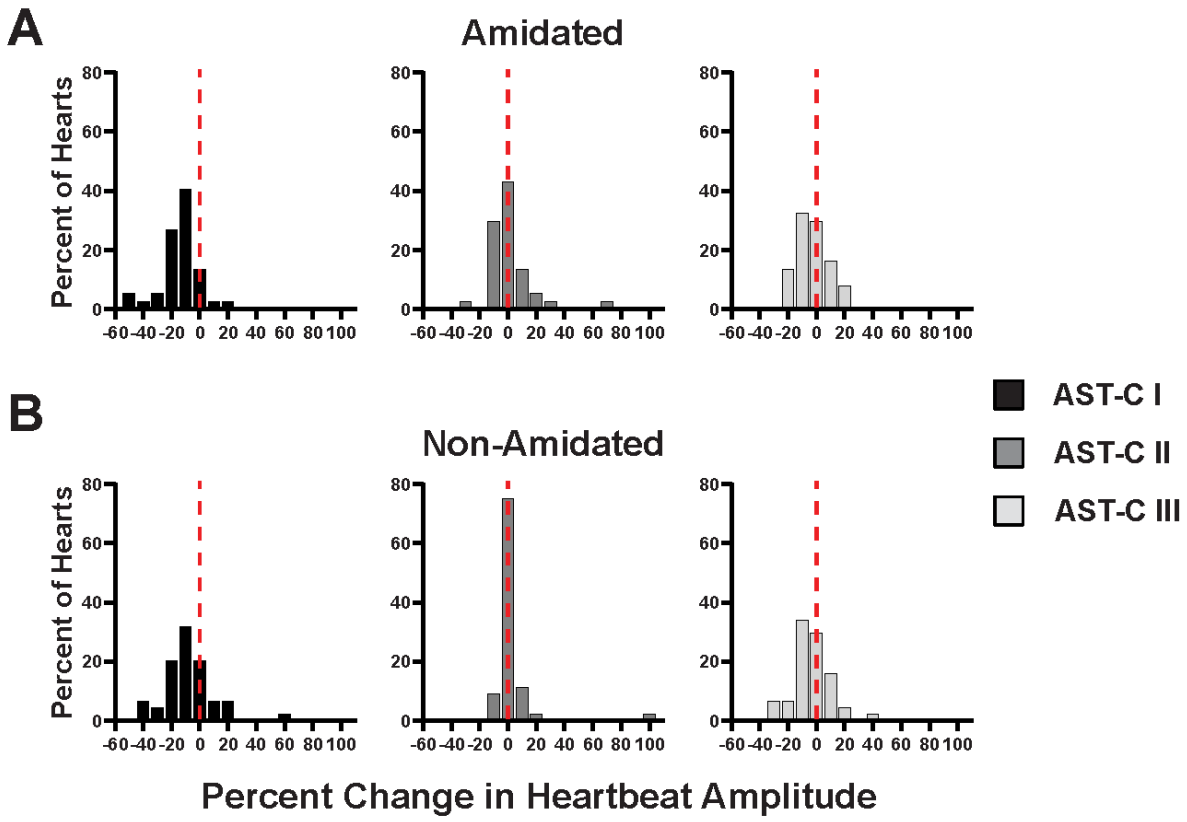

Figure 4. Distributions of changes in heart contraction amplitude elicited by amidated (A) and non-amidated (B) AST-C isoforms. **(A)** Histograms of the change in heartbeat amplitude from control (saline) for each amidated AST-C isoform. AST-C isoforms variably affected heartbeat amplitude, though AST-C I altered amplitude more so than II or III (AST-C I: -13.69 ± 13.9 g, AST-C II: 1.22 ± 15.3 g, AST-C III: -2.90 ± 10.9 g; RM-ANOVA: $p < 0.0001$; Bonferroni post-hoc: I vs II: $p < 0.0001$; I vs III: $p = 0.001$; II vs III: $p = 0.57$; $N = 37$). Distributions were compared using pairwise two-way KS tests: AST-C I vs. II: $p = 3.6\text{x}10^{-7}$; I vs. III: $p = 0.05$; II vs. III: $p = 5.8\text{x}10^{-5}$. **(B)** Same as (**A**) but showing changes in heartbeat amplitude in response to non-amidated AST-C isoforms. For non-amidated isoforms, only the heartbeat response to AST-C I was different from II (AST-C I: -7.42 ± 17.8 g, AST-C II: 2.47 ± 16.1 g, AST-C III: -3.44 ± 13.3 g; RM-ANOVA: $p = 0.005$; Bonferroni post-hoc: I vs II: $p = 0.016$; I vs III: $p = 0.44$; II vs III: $p = 0.018$; $N = 44$). Distributions were compared using pairwise two-way KS tests: AST-C I vs. II: $p = 1.7\text{x}10^{-6}$; I vs. III: $p = 0.32$; II vs. III: $p = 0.002$. Each AST-C isoform was compared pairwise between amidated and non-amidated versions and none of the AST-C isoforms showed differences in force amplitude due to amidation (AST-C I: amidated: -9.84 ± 19.5, non-amidated: -7.43 ± 17.6; paired *t*-test: $p = 0.37$, $N = 47$; AST-C II: amidated: 2.77 ± 14.9, non-amidated: 2.45 ± 16.0; paired *t*-test: $p = 0.92$, $N = 45$; AST-C III: amidated: -2.96 ± 10.8, non-amidated: -4.83 ± 12.4; paired *t*-test: $p = 0.28$, $N = 38$). Distributions of amidated and non-amidated versions of AST-C were not different (AST-C I: two-sample KS test: $p = 0.64$, $N = 47$; AST-C II: two-sample KS test: $p = 0.44$, $N = 45$; AST-C III: two-sample KS test: $p = 0.87$, $N = 38$).

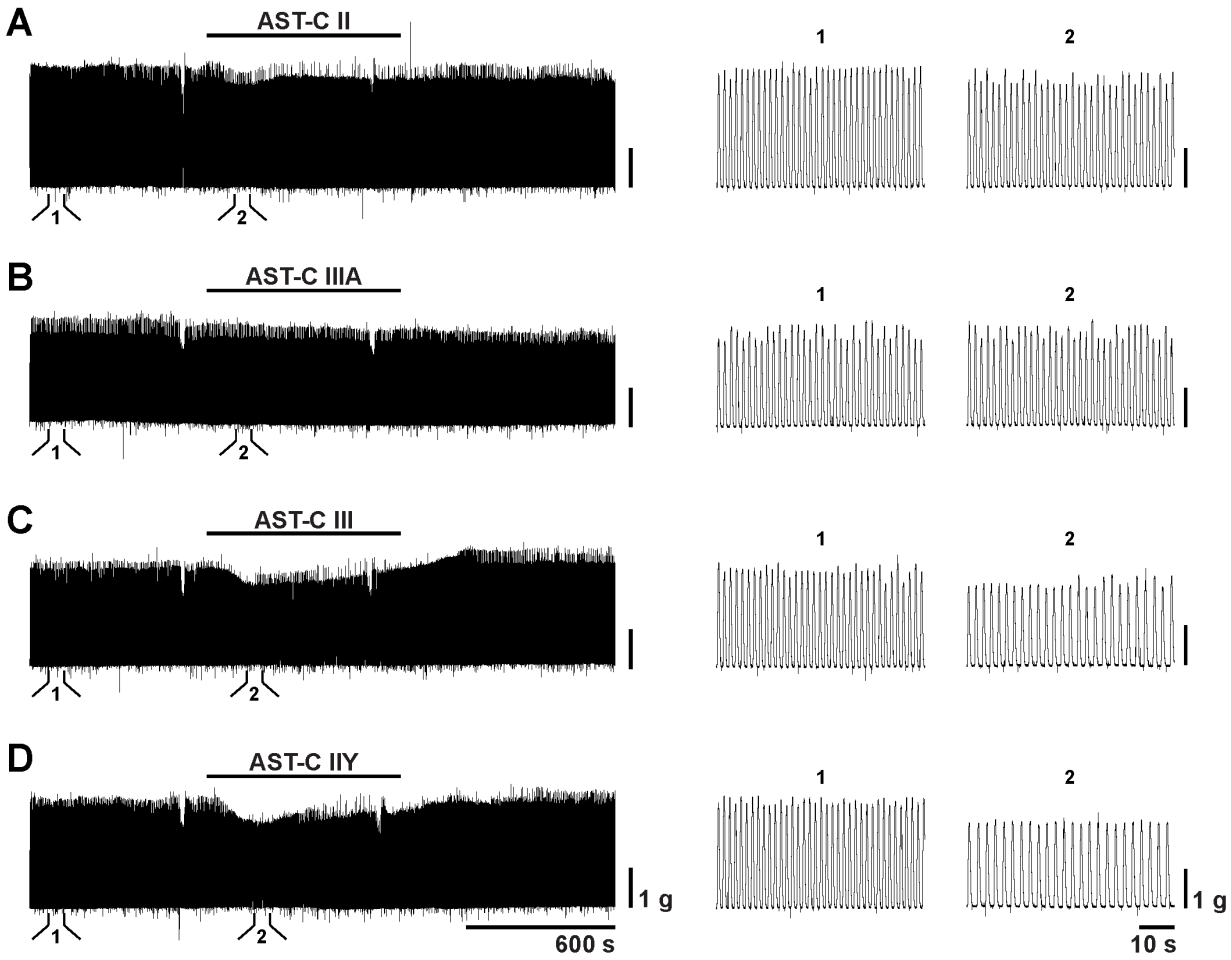

Figure 5. Compressed heartbeat recordings in response to AST-C endogenous (AST-C II & AST-C III) and synthetic (AST-C II Y & AST-C III A) isoforms. All recordings are from the same heart. Black bars indicate peptide perfusion duration. Heartbeat recordings (left) show the heartbeat envelope before, during, and after AST-C application. Recordings to the right of each compressed trace show expanded excerpts of the heartbeat 1) in saline and 2) during the peak response of each AST-C application. Note the similarities in heartbeat response to AST-C II and III A and between AST-C II Y and III.

Figure 6. Distributions of changes in heartbeat frequency in response to endogenous and synthetic AST-C isoforms. (A) Shows the two frequency distributions of AST-C II (top) (endogenous; -5.41 ± 13.0 Hz) and AST-C II Y (bottom) (synthetic; -18.44 ± 13.9 Hz). Values are mean ± SD. Replacing the first alanine within the conserved portion of the AST-C II sequence with a tyrosine (AST-C II Y) resulted in a greater decrease in heartbeat frequency (paired *t*-test: $p = 9.4 \times 10^{-6}$) and altered the overall distribution (two-sample KS test: $p = 5.8 \times 10^{-7}$). **(B)** Shows the two frequency distributions of AST-C III A (top) (synthetic; 0.55 ± 4.7 Hz) and AST-C III (bottom) (endogenous; -18.50 ± 16.4 Hz). Replacing the tyrosine within the conserved portion of the AST-C III sequence with alanine (AST-C III A) resulted in a greater decrease in heartbeat frequency (paired *t*-test: $p = 9.7 \times 10^{-9}$) and altered the overall distribution (two-sample KS test: $p = 1.6 \times 10^{-12}$). Although heartbeat frequency was similar when alanine was replaced with tyrosine in AST-C II (AST-C II Y) compared to AST-C III (paired *t*-test: $p = 1$; two-sample KS test: $p = 1$), replacing the tyrosine in AST-C III with alanine (AST-C III A) resulted in a different heartbeat frequency compared with AST-C II (paired *t*-test: $p = 0.007$; two-sample KS test: $p = 0.01$). All conditions were replicated across all preparations and all frequency values reported are mean ± SD. $N = 47$.

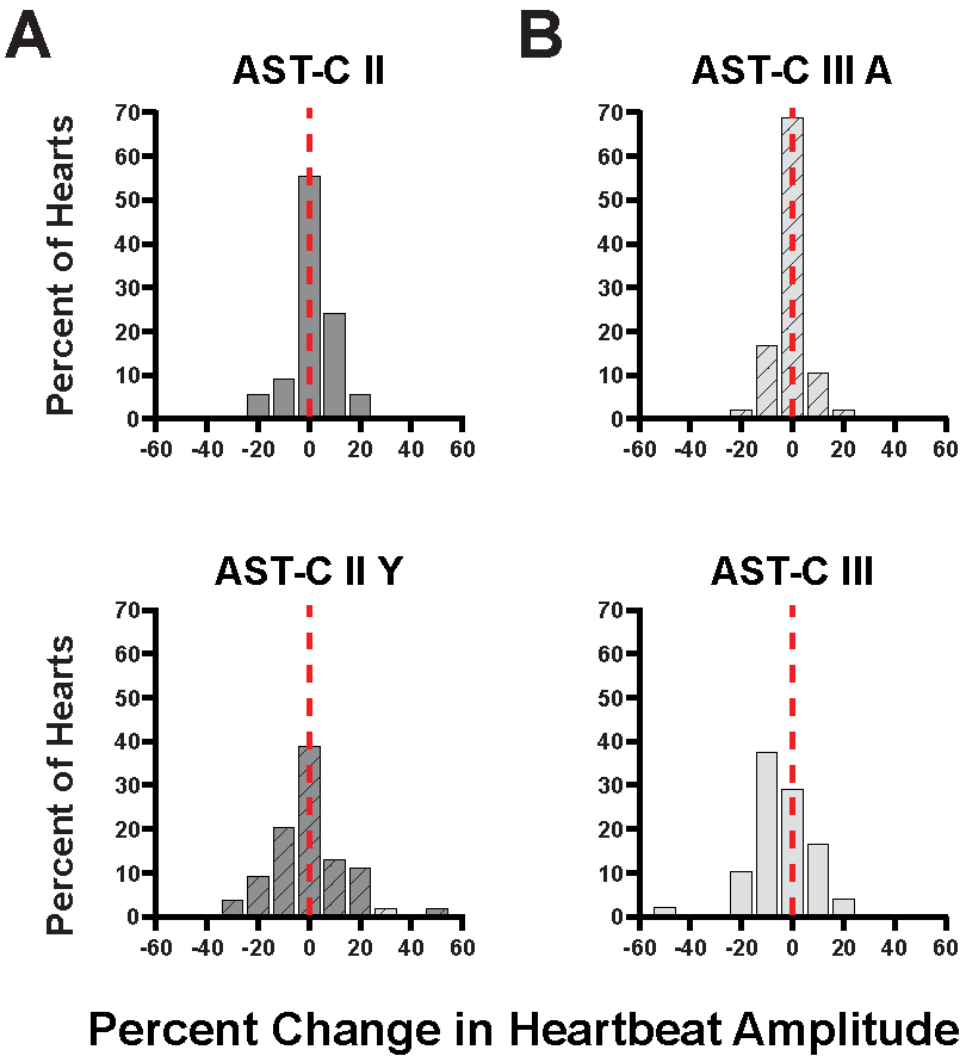

Figure 7. Distributions of changes in heartbeat amplitude in response to endogenous and synthetic AST-C isoforms. (A) Shows the two frequency distributions of AST-C II (top) (endogenous; 0.74 ± 8.8 g) and AST-C II Y (bottom) (synthetic; 1.93 ± 14.3 g). Replacing the first alanine within the conserved portion of the AST-C II sequence with tyrosine (AST-C II Y) did not alter either the amplitude of heartbeat force (paired *t*-test: $p = 1$) or the overall distribution (two-sample KS test: $p = 1$). **(B)** Shows the distributions of changes in contraction amplitude due to perfusion of AST-C III A (top) (synthetic; -0.60 ± 5.4 g) and AST-C III (bottom) (endogenous; -4.08 ± 10.6 g). Replacing the tyrosine within the conserved portion of the AST-C III sequence with alanine (AST-C III A) did not alter heartbeat force amplitude (paired *t*-test: $p = 0.16$) but it did change the overall distribution (two-sample KS test: $p = 0.002$). Although contraction amplitude was different when alanine was replaced with tyrosine in AST-C II (AST-C II Y) compared to AST-C III (paired *t*-test: $p = 0.01$; two-sample KS test: $p = 0.31$), replacing the tyrosine in AST-C III with alanine (AST-C III A) resulted in a contraction amplitude similar to that of AST-C II (paired *t*-test: $p = 1$; two-sample KS test: $p = 1$). All conditions were replicated across all preparations and all amplitude values reported are mean ± SD. $N = 47$.